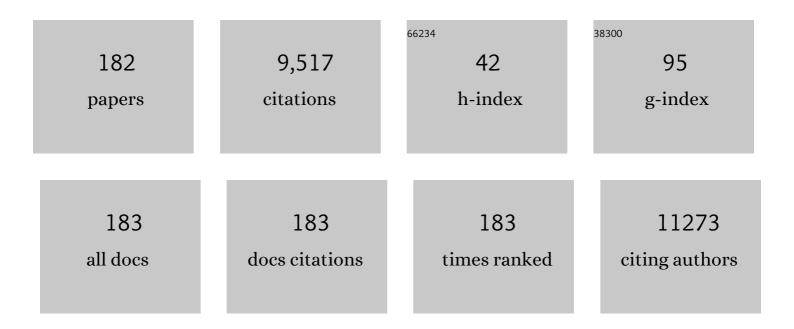
List of Publications by Year in descending order

Source: https://exaly.com/author-pdf/9574733/publications.pdf Version: 2024-02-01



#	Article	IF	CITATIONS
1	Allâ€Dielectric Metaâ€Optics for Highâ€Efficiency Independent Amplitude and Phase Manipulation. Advanced Photonics Research, 2022, 3, .	1.7	10
2	Terahertz bound state in the continuum in dielectric membrane metasurfaces. New Journal of Physics, 2022, 24, 053010.	1.2	3
3	Gold Ion Beam Milled Gold Zero-Mode Waveguides. Nanomaterials, 2022, 12, 1755.	1.9	2
4	Topology-empowered membrane devices for terahertz photonics. Advanced Photonics, 2022, 4, .	6.2	13
5	Demonstration of Large-Size Vertical Ga <sub>2</sub> O <sub>3</sub> Schottky Barrier Diodes. IEEE Transactions on Power Electronics, 2021, 36, 41-44.	5.4	38
6	Topology-controlled Polarized Photoluminescence from Rare-earth Doped Nanocrystals. , 2021, , .		0
7	Kilovolt Tri-Gate GaN Junction HEMTs with High Thermal Stability. , 2021, , .		6
8	Large-Scale Metasurfaces Based on Grayscale Nanosphere Lithography. ACS Photonics, 2021, 8, 1824-1831.	3.2	24
9	Large area vertical Ga2O3 Schottky diodes for X-ray detection. Nuclear Instruments and Methods in Physics Research, Section A: Accelerators, Spectrometers, Detectors and Associated Equipment, 2021, 1013, 165664.	0.7	4
10	Mieâ€Resonant Membrane Huygens' Metasurfaces. Advanced Functional Materials, 2020, 30, 1906851.	7.8	52
11	Tri-gate GaN junction HEMT. Applied Physics Letters, 2020, 117, .	1.5	29
12	Piezoelectric Actuation of Graphene-Coated Polar Structures. IEEE Transactions on Ultrasonics, Ferroelectrics, and Frequency Control, 2020, 67, 2142-2147.	1.7	4
13	Flat optics for image differentiation. Nature Photonics, 2020, 14, 316-323.	15.6	311
14	High-efficiency solar thermophotovoltaic system using a nanostructure-based selective emitter. Solar Energy, 2020, 197, 538-545.	2.9	81
15	To switch or not to switch – a machine learning approach for ferroelectricity. Nanoscale Advances, 2020, 2, 2063-2072.	2.2	12
16	Topological nanophotonics for photoluminescence control. Nanophotonics, 2020, 10, 435-441.	2.9	16
17	Ultra-Sensitive and High Figure of Merit Interferometric Biosensors Using Dispersion Effects in Porous Waveguides. , 2020, , .		1
18	Consideration of temperature-dependent emissivity of selective emitters in thermophotovoltaic systems. Applied Optics, 2020, 59, 5457.	0.9	3

#	Article	IF	CITATIONS
19	Multifunctional metaoptics based on bilayer metasurfaces. Light: Science and Applications, 2019, 8, 80.	7.7	130
20	Surface-Enhanced Raman Scattering (SERS) Studies of Disc-on-Pillar (DOP) Arrays: Contrasting Enhancement Factor with Analytical Performance. Applied Spectroscopy, 2019, 73, 665-677.	1.2	2
21	Dielectric Broadband Metasurfaces for Fiber Modeâ€Multiplexed Communications. Advanced Optical Materials, 2019, 7, 1801679.	3.6	20
22	Environmental Gating and Galvanic Effects in Single Crystals of Organic–Inorganic Halide Perovskites. ACS Applied Materials & Interfaces, 2019, 11, 14722-14733.	4.0	14
23	Nonlinear light generation in topological nanostructures. Nature Nanotechnology, 2019, 14, 126-130.	15.6	187
24	Disorder-Robust Nonlinear Light Generation in Topological Nanostructures. , 2019, , .		1
25	Photonic crystal nanobeam biosensors based on porous silicon. Optics Express, 2019, 27, 9536.	1.7	36
26	Single-mode porous silicon waveguide interferometers with unity confinement factors for ultra-sensitive surface adlayer sensing. Optics Express, 2019, 27, 22485.	1.7	16
27	Noninteracting Multilayer Dielectric Metasurfaces for Multiwavelength Metaoptics. , 2019, , .		Ο
28	Direct atomic fabrication and dopant positioning in Si using electron beams with active real-time image-based feedback. Nanotechnology, 2018, 29, 255303.	1.3	46
29	Grating-based holographic diffraction methods for X-rays and neutrons: phase object approximation and dynamical theory. Journal of Applied Crystallography, 2018, 51, 68-75.	1.9	2
30	Multilayer Noninteracting Dielectric Metasurfaces for Multiwavelength Metaoptics. Nano Letters, 2018, 18, 7529-7537.	4.5	187
31	Quantum metasurface for multiphoton interference and state reconstruction. Science, 2018, 361, 1104-1108.	6.0	227
32	Dynamic transmission control based on all-dielectric Huygens metasurfaces. Optica, 2018, 5, 787.	4.8	116
33	Label-free detection of Herceptin® using suspended silicon microring resonators. Sensors and Actuators B: Chemical, 2018, 275, 394-401.	4.0	17
34	Zika virus detection using antibody-immobilized disposable cover glass and AlGaN/GaN high electron mobility transistors. Applied Physics Letters, 2018, 113, .	1.5	27
35	Nonlinear Wavefront Control with All-Dielectric Metasurfaces. Nano Letters, 2018, 18, 3978-3984.	4.5	180
36	Transparent Dielectric Metasurfaces for Spatial Mode Multiplexing. Laser and Photonics Reviews, 2018, 12, 1800031.	4.4	37

#	Article	IF	CITATIONS
37	Shaping the third-harmonic radiation from silicon nanodimers. Nanoscale, 2017, 9, 2201-2206.	2.8	50
38	Edge States and Topological Phase Transitions in Chains of Dielectric Nanoparticles. Small, 2017, 13, 1603190.	5.2	77
39	Metasurface polarization splitter. Philosophical Transactions Series A, Mathematical, Physical, and Engineering Sciences, 2017, 375, 20160072.	1.6	23
40	Ultrafast charge and energy exchanges at hybrid interfaces involving 2D semiconductors (Conference) Tj ETQq0	0 0 rgBT /	Overlock 10 1
41	Quantification of in-contact probe-sample electrostatic forces with dynamic atomic force microscopy. Nanotechnology, 2017, 28, 065704.	1.3	43
42	Surface Modification of Silicon Pillar Arrays To Enhance Fluorescence Detection of Uranium and DNA. ACS Omega, 2017, 2, 7313-7319.	1.6	6
43	Improvement of Ohmic contacts on Ga2O3 through use of ITO-interlayers. Journal of Vacuum Science and Technology B:Nanotechnology and Microelectronics, 2017, 35, .	0.6	42
44	Atom-by-atom fabrication by electron beam via induced phase transformations. MRS Bulletin, 2017, 42, 653-659.	1.7	18
45	Ohmic contacts on n-type β-Ga2O3 using AZO/Ti/Au. AIP Advances, 2017, 7, .	0.6	48
46	Dimensionality Effects in FeGe2 Nanowires: Enhanced Anisotropic Magnetization and Anomalous Electrical Transport. Scientific Reports, 2017, 7, 7126.	1.6	9
47	AlGaN/GaN High Electron Mobility Transistor Grown and Fabricated on ZrTi Metallic Alloy Buffer Layers. ECS Journal of Solid State Science and Technology, 2017, 6, S3078-S3080.	0.9	2
48	Highest efficiency grayscale all-dielectric meta-holograms. , 2017, , .		0
49	Quantum polarization tomography with all-dielectric metasurfaces. , 2017, , .		0
50	Quantum imaging with dielectric metasurfaces for multi-photon polarization tomography. , 2017, , .		2
51	Third-Harmonic Generation from Photonic Topological States in Zigzag Arrays of Silicon Nanodisks. , 2017, , .		2
52	Quantum tomography with all-dielectric metasurfaces. , 2017, , .		1
53	Broadband transparent all-dielectric metasurfaces. , 2017, , .		0
54	Grayscale transparent metasurface holograms. Optica, 2016, 3, 1504.	4.8	290

#	Article	IF	CITATIONS
55	Lithographyâ€Free Largeâ€Area Metamaterials for Stable Thermophotovoltaic Energy Conversion. Advanced Optical Materials, 2016, 4, 671-676.	3.6	23
56	Evaluation of AlGaN/GaN high electron mobility transistors grown on ZrTi buffer layers with sapphire substrates. Journal of Vacuum Science and Technology B:Nanotechnology and Microelectronics, 2016, 34, 051208.	0.6	4
57	Effect of proton irradiation dose on InAlN/GaN metal-oxide semiconductor high electron mobility transistors with Al2O3 gate oxide. Journal of Vacuum Science and Technology B:Nanotechnology and Microelectronics, 2016, 34, .	0.6	15
58	Invited Article: Broadband highly efficient dielectric metadevices for polarization control. APL Photonics, 2016, 1, .	3.0	320
59	Retention in Porous Layer Pillar Array Planar Separation Platforms. Analytical Chemistry, 2016, 88, 8741-8748.	3.2	14
60	Performance Characteristics of Bio-Inspired Metal Nanostructures as Surface-Enhanced Raman Scattered (SERS) Substrates. Applied Spectroscopy, 2016, 70, 1432-1445.	1.2	5
61	Ultrafast Dynamics of Metal Plasmons Induced by 2D Semiconductor Excitons in Hybrid Nanostructure Arrays. ACS Photonics, 2016, 3, 2389-2395.	3.2	42
62	Exploring Polarization Rotation Instabilities in Superâ€Tetragonal BiFeO <sub>3</sub> Epitaxial Thin Films and Their Technological Implications. Advanced Electronic Materials, 2016, 2, 1600307.	2.6	9
63	Two-dimensional GaSe/MoSe <sub>2</sub> misfit bilayer heterojunctions by van der Waals epitaxy. Science Advances, 2016, 2, e1501882.	4.7	239
64	Slow light Mach–Zehnder interferometer as label-free biosensor with scalable sensitivity. Optics Letters, 2016, 41, 753.	1.7	52
65	Thickness-dependent charge transport in few-layer MoS <sub>2</sub> field-effect transistors. Nanotechnology, 2016, 27, 165203.	1.3	124
66	Direct Measurement of Optical Force Induced by Near-Field Plasmonic Cavity Using Dynamic Mode AFM. Scientific Reports, 2015, 5, 16216.	1.6	21
67	Effect of proton irradiation energy on AlGaN/GaN metal-oxide semiconductor high electron mobility transistors. Journal of Vacuum Science and Technology B:Nanotechnology and Microelectronics, 2015, 33, 051208.	0.6	9
68	Thickness, humidity, and polarization dependent ferroelectric switching and conductivity in Mg doped lithium niobate. Journal of Applied Physics, 2015, 118, .	1.1	17
69	Controlled Nanopatterning of a Polymerized Ionic Liquid in a Strong Electric Field. Advanced Functional Materials, 2015, 25, 805-811.	7.8	13
70	Differentiating Ferroelectric and Nonferroelectric Electromechanical Effects with Scanning Probe Microscopy. ACS Nano, 2015, 9, 6484-6492.	7.3	231
71	Nanopillar Based Enhanced-Fluorescence Detection of Surface-Immobilized Beryllium. Analytical Chemistry, 2015, 87, 6814-6821.	3.2	6

#	Article	IF	CITATIONS
73	Optical and infrared properties of glancing angle-deposited nanostructured tungsten films. Optics Letters, 2015, 40, 506.	1.7	1
74	Probing Local Bias-Induced Transitions Using Photothermal Excitation Contact Resonance Atomic Force Microscopy and Voltage Spectroscopy. ACS Nano, 2015, 9, 1848-1857.	7.3	37
75	Bias assisted scanning probe microscopy direct write lithography enables local oxygen enrichment of lanthanum cuprates thin films. Nanotechnology, 2015, 26, 325302.	1.3	1
76	Study of the effects of GaN buffer layer quality on the dc characteristics of AlGaN/GaN high electron mobility transistors. Journal of Vacuum Science and Technology B:Nanotechnology and Microelectronics, 2015, 33, .	0.6	2
77	Nanoscale pillar arrays for separations. Analyst, The, 2015, 140, 3347-3351.	1.7	9
78	Enhanced absorption in two-dimensional materials via Fano-resonant photonic crystals. Applied Physics Letters, 2015, 106, .	1.5	86
79	Degradation mechanisms of Ti/Al/Ni/Au-based Ohmic contacts on AlGaN/GaN HEMTs. Journal of Vacuum Science and Technology B:Nanotechnology and Microelectronics, 2015, 33, .	0.6	6
80	Large-Scale All-Dielectric Metamaterial Perfect Reflectors. ACS Photonics, 2015, 2, 692-698.	3.2	282
81	Optical diffraction properties of multimicrogratings. Applied Optics, 2015, 54, 1808.	0.9	4
82	Nonlinear Fano-Resonant Dielectric Metasurfaces. Nano Letters, 2015, 15, 7388-7393.	4.5	474
83	Nonlinear Conversion Using Fano-Resonant All-Dielectric Metasurfaces. , 2015, , .		Ο
84	Dielectric Metasurface Analogue of Electromagnetically Induced Transparency. , 2015, , .		2
85	Improvement of drain breakdown voltage with a back-side gate on AlGaN/GaN high electron mobility transistors. Journal of Vacuum Science and Technology B:Nanotechnology and Microelectronics, 2015, 33, 042201.	0.6	4
86	On Field-Effect Photovoltaics: Gate Enhancement of the Power Conversion Efficiency in a Nanotube/Silicon-Nanowire Solar Cell. ACS Applied Materials & Interfaces, 2015, 7, 21182-21187.	4.0	11
87	Ion transport and softening in a polymerized ionic liquid. Nanoscale, 2015, 7, 947-955.	2.8	18
88	Effect of low dose Î <sup>3</sup> -irradiation on DC performance of circular AlGaN/GaN high electron mobility transistors. Journal of Vacuum Science and Technology B:Nanotechnology and Microelectronics, 2014, 32, .	0.6	20
89	Suspended micro-ring resonator for enhanced biomolecule detection sensitivity. , 2014, , .		5
90	All-dielectric metasurface analogue of electromagnetically induced transparency. Nature Communications, 2014, 5, 5753.	5.8	823

#	Article	IF	CITATIONS
91	Growth of skyrmionic MnSi nanowires on Si: Critical importance of the SiO2 layer. Nano Research, 2014, 7, 1788-1796.	5.8	11
92	Effect of Gamma Irradiation on DC Performance of Circular-Shaped AlGaN/GaN High Electron Mobility Transistors. ECS Transactions, 2014, 61, 205-210.	0.3	1
93	Exploring Local Electrostatic Effects with Scanning Probe Microscopy: Implications for Piezoresponse Force Microscopy and Triboelectricity. ACS Nano, 2014, 8, 10229-10236.	7.3	123
94	Cavitation on Deterministically Nanostructured Surfaces in Contact with an Aqueous Phase: A Small-Angle Neutron Scattering Study. Langmuir, 2014, 30, 9985-9990.	1.6	10
95	Dielectric Meta-Reflectarray for Broadband Linear Polarization Conversion and Optical Vortex Generation. Nano Letters, 2014, 14, 1394-1399.	4.5	877
96	Enhancing the Sensitivity of Label-Free Silicon Photonic Biosensors through Increased Probe Molecule Density. ACS Photonics, 2014, 1, 590-597.	3.2	41
97	Direct Probing of Charge Injection and Polarizationâ€Controlled Ionic Mobility on Ferroelectric LiNbO <sub>3</sub> Surfaces. Advanced Materials, 2014, 26, 958-963.	11.1	49
98	Characteristics of gate leakage current and breakdown voltage of AlGaN/GaN high electron mobility transistors after postprocess annealing. Journal of Vacuum Science and Technology B:Nanotechnology and Microelectronics, 2014, 32, .	0.6	15
99	Controlled Vapor Phase Growth of Single Crystalline, Two-Dimensional GaSe Crystals with High Photoresponse. Scientific Reports, 2014, 4, 5497.	1.6	222
100	A new approach for probing matter in periodic nanoconfinements using neutron scattering. Journal of Applied Crystallography, 2014, 47, 1367-1373.	1.9	4
101	Space- and Time-Resolved Mapping of Ionic Dynamic and Electroresistive Phenomena in Lateral Devices. ACS Nano, 2013, 7, 6806-6815.	7.3	48
102	Probing Local Ionic Dynamics in Functional Oxides at the Nanoscale. Nano Letters, 2013, 13, 3455-3462.	4.5	55
103	Silicon Nanopillars As a Platform for Enhanced Fluorescence Analysis. Analytical Chemistry, 2013, 85, 9031-9038.	3.2	29
104	Realization of an all-dielectric zero-index optical metamaterial. Nature Photonics, 2013, 7, 791-795.	15.6	589
105	The effects of proton irradiation on the reliability of InAlN/GaN high electron mobility transistors. Proceedings of SPIE, 2013, , .	0.8	1
106	Surface-Induced Orientation Control of CuPc Molecules for the Epitaxial Growth of Highly Ordered Organic Crystals on Graphene. Journal of the American Chemical Society, 2013, 135, 3680-3687.	6.6	125
107	Casimir forces on a silicon micromechanical chip. Nature Communications, 2013, 4, 1845.	5.8	109

108 A robust VACNF platform for electrochemical biosensor. , 2013, , .

#	Article	IF	CITATIONS
109	Effect of buffer structures on AlGaN/GaN high electron mobility transistor reliability. Journal of Vacuum Science and Technology B:Nanotechnology and Microelectronics, 2013, 31, 011805.	0.6	16
110	GaN metal–insulator–semiconductor high-electron-mobility transistor with plasma enhanced atomic layer deposited AlN as gate dielectric and passivation. Journal of Vacuum Science and Technology B:Nanotechnology and Microelectronics, 2013, 31, 052201.	0.6	6
111	Impact of proton irradiation on dc performance of AlGaN/GaN high electron mobility transistors. Journal of Vacuum Science and Technology B:Nanotechnology and Microelectronics, 2013, 31, 042202.	0.6	23
112	Growth diagram of La0.7Sr0.3MnO3 thin films using pulsed laser deposition. Journal of Applied Physics, 2013, 113, .	1.1	20
113	Dependence on proton energy of degradation of AlGaN/GaN high electron mobility transistors. Journal of Vacuum Science and Technology B:Nanotechnology and Microelectronics, 2013, 31, .	0.6	34
114	In Situ Formation of Micron-Scale Li-Metal Anodes with High Cyclability. ECS Electrochemistry Letters, 2013, 3, A4-A7.	1.9	4
115	SnO2-gated AlGaN/GaN high electron mobility transistors based oxygen sensors. Journal of Vacuum Science and Technology B:Nanotechnology and Microelectronics, 2012, 30, .	0.6	5
116	Effects of semiconductor processing chemicals on conductivity of graphene. Journal of Vacuum Science and Technology B:Nanotechnology and Microelectronics, 2012, 30, .	0.6	7
117	Quenching of initial ac susceptibility in single-domain Ni nanobars. Physical Review B, 2012, 85, .	1.1	2
118	Proton irradiation energy dependence of dc and rf characteristics on InAlN/GaN high electron mobility transistors. Journal of Vacuum Science and Technology B:Nanotechnology and Microelectronics, 2012, 30, 041206.	0.6	9
119	Silicon Nanopillars for Field-Enhanced Surface Spectroscopy. ACS Nano, 2012, 6, 2948-2959.	7.3	75
120	Doping-Based Stabilization of the M2 Phase in Free-Standing VO <sub>2</sub> Nanostructures at Room Temperature. Nano Letters, 2012, 12, 6198-6205.	4.5	145
121	UV ozone treatment for improving contact resistance on graphene. Journal of Vacuum Science and Technology B:Nanotechnology and Microelectronics, 2012, 30, .	0.6	36
122	Nanotransfer Printing Using Plasma Etched Silicon Stamps and Mediated by in Situ Deposited Fluoropolymer. Journal of the American Chemical Society, 2011, 133, 7722-7724.	6.6	12
123	Nonlinear Phenomena in Multiferroic Nanocapacitors: Joule Heating and Electromechanical Effects. ACS Nano, 2011, 5, 9104-9112.	7.3	69
124	Low-Voltage, Low-Power, Organic Light-Emitting Transistors for Active Matrix Displays. Science, 2011, 332, 570-573.	6.0	466
125	Stamping plasmonic nanoarrays on SERSâ€supporting platforms. Journal of Raman Spectroscopy, 2011, 42, 1916-1924.	1.2	13
126	Comparison of DC performance of Pt/Ti/Au- and Ni/Au-gated AlGaN/GaN high electron mobility transistors. Journal of Vacuum Science and Technology B:Nanotechnology and Microelectronics, 2011, 29, 042202.	0.6	3

#	Article	IF	CITATIONS
127	A half wave retarder made of bilayer subwavelength metallic apertures. Applied Physics Letters, 2011, 98, 151107.	1.5	9
128	Fabrication of InAlAs/InGaAsSb/InGaAs double heterojunction bipolar transistors. Journal of Vacuum Science and Technology B:Nanotechnology and Microelectronics, 2011, 29, 031205.	0.6	6
129	Improvement of Off-State Stress Critical Voltage by Using Pt-Gated AlGaN/GaN High Electron Mobility Transistors. Electrochemical and Solid-State Letters, 2011, 14, H264.	2.2	21
130	Effects of proton irradiation on dc characteristics of InAlN/GaN high electron mobility transistors. Journal of Vacuum Science and Technology B:Nanotechnology and Microelectronics, 2011, 29, 061201.	0.6	17
131	Improved Off-State Stress Critical Voltage on AlGaN/GaN High Electron Mobility Transistors Utilizing Pt/Ti/Au Based Gate Metallization. ECS Transactions, 2011, 41, 63-70.	0.3	3
132	Fabrication and Characterization of Self-Aligned InAlAs/InGaAsSb/InGaAs Double Heterojunction Bipolar Transistors. ECS Transactions, 2011, 41, 117-127.	0.3	0
133	ON-SKY DEMONSTRATION OF A LINEAR BAND-LIMITED MASK WITH APPLICATION TO VISUAL BINARY STARS. Astrophysical Journal, 2010, 715, 1533-1538.	1.6	12
134	Normallyâ€on/off AlN/GaN high electron mobility transistors. Physica Status Solidi C: Current Topics in Solid State Physics, 2010, 7, 2415-2418.	0.8	5
135	Passivation of AlNâ^•GaN high electron mobility transistor using ozone treatment. Journal of Vacuum Science and Technology B:Nanotechnology and Microelectronics, 2010, 28, 52-55.	0.6	4
136	Isolation blocking voltage of nitrogen ion-implanted AlGaN/GaN high electron mobility transistor structure. Applied Physics Letters, 2010, 97, .	1.5	49
137	Optical transmission through double-layer, laterally shifted metallic subwavelength hole arrays. Optics Letters, 2010, 35, 2124.	1.7	16
138	Proton irradiation effects on Sb-based heterojunction bipolar transistors. Journal of Vacuum Science & Technology B, 2009, 27, L33.	1.3	1
139	Development of enhancement mode AlN/GaN high electron mobility transistors. Applied Physics Letters, 2009, 94, .	1.5	49
140	Indium zinc oxide thin films deposited by sputtering at room temperature. Applied Surface Science, 2008, 254, 2878-2881.	3.1	32
141	Ir Diffusion Barriers in Ni/Au Ohmic Contacts to p-Type CuCrO2. Journal of Electronic Materials, 2008, 37, 161-166.	1.0	1
142	High temperature Ohmic contacts to p-type GaN for use in light emitting applications. Physica Status Solidi C: Current Topics in Solid State Physics, 2008, 5, 2241-2243.	0.8	0
143	RF-sputtered CrB2 diffusion barrier for Ni/Au Ohmic contacts on p-CuCrO2. Applied Surface Science, 2008, 254, 5211-5215.	3.1	2
144	High-Performance Indium Gallium Zinc Oxide Transparent Thin-Film Transistors Fabricated by Radio-Frequency Sputtering. Journal of the Electrochemical Society, 2008, 155, H383.	1.3	94

#	Article	IF	CITATIONS
145	Stable room temperature deposited amorphous InGaZnO[sub 4] thin film transistors. Journal of Vacuum Science & Technology B, 2008, 26, 959.	1.3	66
146	Irâ^•Au Ohmic Contacts on Bulk, Single-Crystal n-Type ZnO. Journal of the Electrochemical Society, 2007, 154, H161.	1.3	2
147	Nanolithographic patterning of transparent, conductive single-walled carbon nanotube films by inductively coupled plasma reactive ion etching. Journal of Vacuum Science & Technology B, 2007, 25, 348.	1.3	47
148	Influence of the film properties on the plasma etching dynamics of rf-sputtered indium zinc oxide layers. Journal of Vacuum Science and Technology A: Vacuum, Surfaces and Films, 2007, 25, 659-665.	0.9	9
149	W 2 B and CrB2 diffusion barriers for Niâ^•Au contacts to p-GaN. Applied Physics Letters, 2007, 91, .	1.5	9
150	Ohmic contacts to p-type GaN based on TaN, TiN, and ZrN. Applied Physics Letters, 2007, 90, 212107.	1.5	17
151	Ir-Based Schottky and Ohmic Contacts on n-GaN. Journal of the Electrochemical Society, 2007, 154, H584.	1.3	4
152	Thermal stability of Ohmic contacts to InN. Applied Physics Letters, 2007, 90, 162107.	1.5	7
153	Room-Temperature-Deposited Indium-Zinc Oxide Thin Films with Controlled Conductivity. Electrochemical and Solid-State Letters, 2007, 10, H267.	2.2	11
154	Room temperature deposited indium zinc oxide thin film transistors. Applied Physics Letters, 2007, 90, 232103.	1.5	132
155	Improved Long-Term Thermal Stability At 350°C Of TiB2–Based Ohmic Contacts On AlGaN/GaN High Electron Mobility Transistors. Journal of Electronic Materials, 2007, 36, 379-383.	1.0	1
156	Thermal Stability of Nitride-Based Diffusion Barriers for Ohmic Contacts to n-GaN. Journal of Electronic Materials, 2007, 36, 1662-1668.	1.0	1
157	The contribution of valence unstable ytterbium states into kinetic properties of YbNi2â^'xGe2+x and YbCu2â^'xSi2+x. Journal of Alloys and Compounds, 2006, 425, 54-58.	2.8	Ο
158	Annealing and measurement temperature dependence of W2B5-based rectifying contacts to n-GaN. Applied Surface Science, 2006, 252, 5814-5819.	3.1	9
159	Use of TiB2 diffusion barriers for Ni/Au ohmic contacts on p-GaN. Applied Surface Science, 2006, 253, 1255-1259.	3.1	11
160	ZrB 2 -based Ohmic contacts to p-GaN. Applied Surface Science, 2006, 253, 1934-1938.	3.1	2
161	ZrB 2 Schottky diode contacts on n-GaN. Applied Surface Science, 2006, 253, 2315-2319.	3.1	14
162	Stability of Ti/Al/ZrB 2 /Ti/Au ohmic contacts on n-GaN. Applied Surface Science, 2006, 253, 2340-2344.	3.1	11

#	Article	IF	CITATIONS
163	ZrB2/Pt/Au Ohmic contacts on bulk, single-crystal ZnO. Applied Surface Science, 2006, 253, 2465-2469.	3.1	6
164	Annealing temperature dependence of TiB2 schottky barrier contacts on n-GaN. Journal of Electronic Materials, 2006, 35, 658-662.	1.0	1
165	Comparison of electrical and reliability performances of TiB[sub 2]-, CrB[sub 2]-, and W[sub 2]B[sub 5]-based Ohmic contacts on n-GaN. Journal of Vacuum Science & Technology B, 2006, 24, 744.	1.3	13
166	Thermally Stable TiB[sub 2] Ohmic Contacts on n-ZnO. Electrochemical and Solid-State Letters, 2006, 9, G164.	2.2	3
167	Improved thermally stable ohmic contacts on p-GaN based on W2B. Applied Physics Letters, 2006, 88, 012104.	1.5	13
168	Thermal stability of W2B and W2B5 contacts on ZnO. Applied Surface Science, 2005, 252, 1846-1853.	3.1	9
169	W2B-based ohmic contacts to n-GaN. Applied Surface Science, 2005, 252, 1826-1832.	3.1	7
170	W2B-based rectifying contacts to n-GaN. Applied Physics Letters, 2005, 87, 052110.	1.5	24
171	CrB[sub 2] Schottky Barrier Contacts on n-GaN. Journal of the Electrochemical Society, 2005, 152, G804.	1.3	9
172	Improved Thermal Stability CrB2Contacts on ZnO. Japanese Journal of Applied Physics, 2005, 44, 7291-7295.	0.8	3
173	Proton induced X-ray emission analysis of aberrant cowrie shells. Nuclear Instruments & Methods in Physics Research B, 2004, 215, 223-227.	0.6	0
174	Effect of deposition conditions and annealing on W Schottky contacts on n-GaN. Materials Science in Semiconductor Processing, 2004, 7, 95-98.	1.9	15
175	Observation of resistance switching between insulating and metallic states in nano-crystalline La0.65Ca0.35MnO3 film. Physica B: Condensed Matter, 2003, 334, 403-407.	1.3	2
176	Some details of the electronic structure of tin oxide films. Physica Status Solidi (B): Basic Research, 2003, 238, 7-10.	0.7	0
177	Transport properties of La1â^'xSrxCoO3â^'δfilms (0.15⩽x⩽0.5). Physica B: Condensed Matter, 2002, 324,	<b>20</b> 5-216.	12
178	Elemental analysis of bone: proton-induced X-ray emission testing in forensic cases. Forensic Science International, 2002, 125, 37-41.	1.3	38
179	Influence of charge ordering and phase separation on transport properties of Pr0.65Ca0.35MnO3 films. Physica B: Condensed Matter, 2001, 307, 239-246.	1.3	7
180	Nature of critical current and coherent phenomena in granular MoNx thin films. Low Temperature Physics, 2000, 26, 881-885.	0.2	2

#	Article	IF	CITATIONS
181	STM studies of the initial stages of growth of Sb on Si(100) surfaces. Surface Science, 1999, 423, 43-52.	0.8	18
182	Atomic manipulation for patterning ultrathin films. Journal of Vacuum Science & Technology an Official Journal of the American Vacuum Society B, Microelectronics Processing and Phenomena, 1995, 13, 2828.	1.6	7